Astronomy & Astrophysics manuscript no. output
July 20, 2024

HI line observations of galaxies with the Nançay Radio Telescope

Adrien Anthore[1]

Master Sciences de l'Univers et Technologies Spatiales de l'Observatoire de Paris-PSL: M1 ⋆

ABSTRACT

We have performed 21 cm H I line observations with the 100 m-class single dish Nançay Radio Telescope of six edge-on Low Surface Brightness (LSB) galaxies and two High Surface Brightness (HSB) galaxies, all with previously reported strong H I lines. Using our measured H I line parameters, and optical and H I line imaging data from the literature, we estimated the dark matter content of the observed galaxies. We found that dark matter represents on average 88±4% of the total mass for the LSB galaxies and 73±5% for the HSB galaxies. This result is consistent with previous studies.

Key words. galaxies: general – radio lines: galaxies

1. Introduction

The main goal of this project is to estimate the dark matter contents of a sample of spiral galaxies using 21 cm H I line spectra which we obtained with the single-dish Nançay Radio Telescope (NRT).

For this purpose, we will estimate their total and their baryonic masses; the difference between those two terms corresponds to an invisible mass component in the galaxies, their dark matter. In order to estimate the total mass we need to determine the maximum rotation speed and the radius of the H I distribution of the galaxies. Their baryonic mass is estimated from the mass of gas and stars in the galaxies.

We mainly selected edge-on spiral galaxies from the Flat Galaxies Catalogue (FGC, Karachentsev et al. 1993 with already known strong H I lines (Matthews & van Driel 2000), to ensure their detection within the allocated NRT telescope time and to directly measure their maximum rotation velocity.

Optical surface photometry has shown (e.g. Matthews 2000; Matthews & Uson 2008) that these are Low Surface Brightness (LSBs) galaxies. We adopt the commonly used definition that LSBs have a central surface brightness at least $1 magarcsec^{-2}$ fainter than the surface brightness of the sky. Most LSB galaxies are low mass, low metallicity and rather blue galaxies with a high mass-to-light ratio (O'Neil, K. et al. 2004). We also observed two High Surface Brightness (HSBs) spiral galaxies, the type that defines the Hubble sequence.

Unless otherwise indicated, all radial velocities are heliocentric and in the optical convention, $cz = c(\lambda - \lambda_0)/\lambda_0$. A standard Hubble constant of 70 km s^{-1} Mpc^{-1} was used throughout the paper.

2. Galaxy selection

We selected galaxies which (1) lie within the RA range accessible within the allocated telescope time, (2) lie within the declination range accessible at Nançay, $\delta \geq -39°$, (3) have known strong H I lines, (4) are preferably edge-on, to measure directly their maximum rotation velocity, and (5) are smaller than the telescope beam size.

The final sample consist of eight galaxies, six edge-on late-morphological type (Scd-Sm) LSB galaxies from the FGC, and two HSB spirals, one edge-on (NGC 3600) and another (NGC 7741) with an inclination of 50°, which had been selected when no suitable FGC candidates were available.

Listed in Table 1 are basic optical properties of the observed galaxies. Unless otherwise indicated, the data were taken from the online databases HyperLeda[1] and NED[2].

- RA, Dec: right ascension and declination of the optical center in epoch J2000.0, taken from the NED database;
- Morph.: morphological type taken from NED, or otherwise from the FGC;
- B_T: total apparent magnitude in the B band, within the 25 mag arcsec^{-2} isophote;
- D_{25}: major axis diameter in the B band, at the 25 mag arcsec^{-2} isophotal level, in $'$;
- b/a: minor-to-major axis ratio in the B band, at the 25 mag arcsec^{-2} isophotal level;
- V_{opt}: heliocentric radial velocity of the galaxy, in km s^{-1}.

3. Observations and data reduction

The Nançay Radio Telescope telescope (NRT) is a 100 m-class meridian transit, single dish-type instrument. It consists of a tiltable plan mirror (200 m long and 40 m high), a spherical mirror (300 m long and 35 m high) and a focal cabin which contains the receivers. The telescope beam size is $3'.5 \times 23'$ (alpha times delta). We made observations simultaneously in two linear polarizations in 4096 frequency channels, resulting in a 2.6 km s^{-1} velocity resolution over the radial velocity range -3239 to 7457 km s^{-1} Flux calibration is performed by frequent insertion of a calibrated noise diode into the beam and regular observations of strong continuum radio sources by NRT staff. The data

⋆ Project supervisors: J.-M. Martin and W. van Driel, GEPI, Observatoire de Paris, Université PSL, CNRS, 5 place Jules Janssen, 92195 Meudon, France

[1] http://leda.univ-lyon1.fr/
[2] https://ned.ipac.caltech.edu

Table 1. Basic optical properties of the observed galaxies

Name	RA (J2000.0)	Dec	Morph.	B_T (mag)	D_{25} (′)	b/a	V_{opt} (km/s)	reference
IC 2267	08 18 01.5	24 44 10	SBcd?	15.20	1.9	0.13	2083	Aihara et al. (2011)
NGC 3600	11 15 52.0	41 35 27	Sa?	12.98	1.9	0.32	703	Alam et al. (2015)
UGC 7170	12 08 04.0	19 06 05	Scd:	14.73	2.8	0.08	2443	Alam et al. (2015)
FGC 1496	12 44 19.1	-05 32 13	Sd:	15.90	1.7	0.10		
FGC 1543	13 02 55.7	55 41 40	Sm	17.04	0.9	0.18	1357	Alam et al. (2015)
ESO 577-038	13 48 25.7	-18 52 20	Sd:	16.61	2.1	0.05		
FGC 1731	14 14 34.1	-04 25 02	Sd	16.50	1.0	0.15		
NGC 7741	23 43 54.4	26 04 32	SBcd	11.82	3.6	0.66	750	Blackman & Pence (1982)

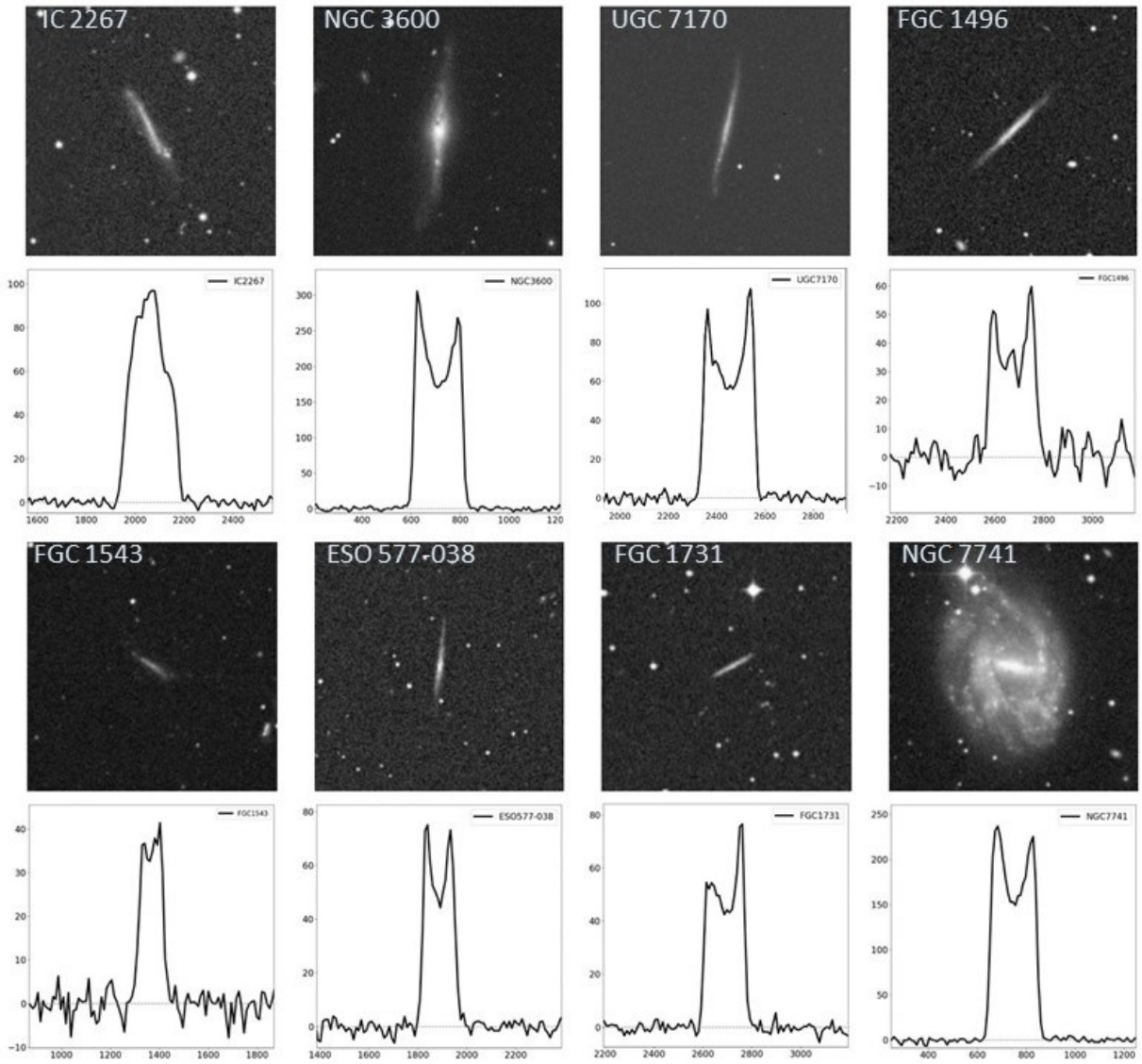

Fig. 1. Pairs of optical images and our Nançay 21 cm H I line spectra for each of the observed galaxies. The optical images are digitized photographic plates in the *B* band from the Digital Sky Survey DSS2, of $5' \times 5'$ in size. The corresponding H I profiles show flux density (in mJy) as a function of radial velocity (in km s^{-1}).

were taken in an equal integration time, on/off-source position-switching mode. The observations were made in October 2022, using a total of about 20 hours of telescope time.

We used standard NRT software SIR to (1) average the data obtained in the two receiver polarizations, (2) convert signal strengths from system temperature to flux density in mJy, (3) fit and subtract polynomial baselines, (4) smooth the data in velocity to a resolution of 10 km s^{-1}, and (5) convert the radial H I velocities (V_{radio}), measured based on frequencies, to the standard optical cz convention (V_{HI}), as $cz = 1/((1/V_{radio}) - (1/c))$ (for further technical details see e.g. van Driel, W. et al. 2016).

Table 2. H I line profile parameters of the observed galaxies

Name	*rms* (mJy)	*SNR*	V_{HI} (km/s)	W_{50} (km/s)	W_{20} (km/s)	F_{HI} (Jy km/s)
IC 2267	1.45	67	2061.0±0.9	190	230	16.3±0.2
NGC 3600	2.34	130	708.5±0.2	199	215	45.6±0.3
UGC 7170	1.91	56	2453.4±0.5	210	229	16.1±0.2
FGC 1496	5.87	10	2671.4±3.1	190	211	8.0±0.6
FGC 1543	2.64	16	1367.5±2.2	100	122	3.4±0.2
ESO 577-038	2.33	32	1886.9±0.9	132	151	8.3±0.2
FGC 1731	1.86	41	2693.0±0.7	161	180	9.1±0.2
NGC 7741	2.47	95	747.4±0.3	191	209	37.6±0.3

Table 3. Estimated global parameters of the observed galaxies

Name	d (Mpc)	$\log(L_B)$ ($L_{\odot,B}$)	$\log(M_\star)$ ($M_\odot$)	$\log(M_{HI})$ ($M_\odot$)	$\log(M_{bar})$ ($M_\odot$)	V_{rot} (km/s)	$\log(M_{tot})$ ($M_\odot$)	M_{tot}/M_{bar}	$DM\%$
IC 2267	29.9	9.11	9.26	9.54	9.82	115	10.79	9	89
NGC 3600	12.6	9.23	9.38	9.23	9.68	108	10.17	3	68
UGC 7170	36.6	9.47	9.62	9.71	10.05	113	11.04	10	90
FGC 1496	38.6	9.05	9.19	9.45	9.74	106	10.80	12	91
FGC 1543	23.2	8.13	8.27	8.63	8.89	61	9.80	8	88
ESO 577-038	27.0	8.54	8.69	9.15	9.39	76	10.44	11	91
FGC 1731	39.6	8.84	8.99	9.53	9.75	90	10.42	5	79
NGC 7741	12.3	9.75	9.90	9.12	9.99	136	10.65	5	78

4. Results

The H I profiles and optical *B* band images of the observed galaxies are shown in Fig. 2.

Listed for each galaxy in Table 2 are the following parameters of their H I line profiles:

- *rms*: rms noise level of the spectrum, in mJy;
- *SNR*: peak signal-to-noise ratio, i.e., the peak flux density divided by the *rms*;
- V_{HI}: mean radial velocity, in km s^{-1};
- W_{50}: line width at 50% of the peak level, in km s^{-1};
- W_{20}: line width at 20% of the peak level, in km s^{-1};
- F_{HI}: integrated line flux, in Jy km s^{-1}.

The uncertainties in V_{HI} and F_{HI} were estimated following Schneider et al. (1990). Uncertainties in W_{50} and W_{20} are, respectively, 2 and 3.1 times those in V_{HI}.

$$\sigma_{V_{HI}} = 1.5(W_{20} - W_{50})/(SNR) \quad (1)$$

$$\sigma_{F_{HI}} = 2.810^{-3} {W_{20}}^{0.5} R^{0.5} rms \quad (2)$$

Where R is the velocity resolution of the spectra, in km s^{-1}.

Listed for each galaxy in Table 3 are our estimated global parameters. For further details on the methodology used, see Section 5.

- d: distance of the galaxy (in Mpc), based on its radial velocity corrected for the infall of the Local Group toward the Virgo cluster and using the Hubble-Lemaître law with a Hubble constant H_0 = 70 km s^{-1} Mpc^{-1};
- L_B: total luminosity in the *B* band (in $L_{\odot,B}$) calculated using B_T corrected for Galactic foreground extinction following Schlafly & Finkbeiner (2011), and assuming a *B* band solar absolute magnitude of 5.48 mag (Allen 1973);
- $M_\star$: total stellar mass (in $M_\odot$), estimated from L_B using a mass-to-luminosity conversion factor of 1.4 $M_\odot/L_{\odot,B}$;
- M_{HI}: total H I mass (in $M_\odot$), $M_{HI} = 2.35610^5 d^2 F_{HI}$;
- M_{bar}: total baryonic mass (in $M_\odot$), $M_{bar} = M_\star + 1.4M_{HI}$;
- V_{rot}: maximum rotation velocity (in km s^{-1}), $V_{rot} = W_{20}/2\sin(i)$;
- M_{tot}: total (dynamical) mass, $M_{tot} = 2.32610^5 {V_{rot}}^2 r_{max}$;
- $DM\%$: percentage of the dark matter contribution to the total mass.

5. Discussion

Distances d were calculated using radial velocities corrected for the infall of the Local Group towards the Virgo cluster, as listed in HyperLeda, and adopting a Hubble constant of H_0 = 70 km s^{-1} Mpc^{-1}. This correction was applied because for galaxies close to the Milky Way local kinematics can have a significant impact on their observed radial velocities. In three cases the corrections were significant, 14-25%

To compute L_B luminosities we did not use the *btc* values from HyperLeda, which are total apparent magnitudes in the *B* band corrected for the extinction due to both the dust inside the galaxy itself as well as in the Milky Way. This correction of on average a factor 5 in luminosity, which was estimated for HSB galaxies, appears significantly overestimated for our galaxies, most of which are LSBs and for which we do not see much dust in optical images (see Fig. 2). The total apparent magnitude we have used therefore includes only a correction to B_T for the Galactic extinction, A_B, estimated as $1.32A_V$ Cardelli et al. (1989) where A_V is the Galactic extinction in the *V* band, as listed in NED.

To estimate the total stellar mass $M_\star$ we used the *B*-band stellar population mass-to-light ratio of 1.4 $M_\odot/L_{\odot,B}$ adopted by McGaugh et al. (2000).

The total baryonic mass $M_{\rm bar}$ was approximated as the sum of $M_\star$ and the total gas mass, which was assumed to be 1.4 times the total H I mass, a standard correction factor to account for Helium gas. We did not take into account the molecular hydrogen gas mass, as it does not appear to be significant in late type galaxies (McGaugh et al. 2000).

The total (dynamical) mass $M_{\rm tot}$ was calculated assuming a simple spherical distribution of dark matter around the galaxy. For the maximum rotation speed $V_{\rm rot}$ of the flat part of the rotation curve of a galaxy we used the common assumption that it corresponds to the W_{20} line width, corrected for the inclination, We based our estimates for the $r_{\rm max}$ radii of the H I distributions on the optical radii of galaxies and their relationship with the radii of their H I distributions, as derived from interferometric H I line imaging observations. For this, the surface brightness nature of the galaxies was taken into account, as the ratio of H I-to-optical radii is different for LSB and HSB galaxies. The H I diameter of a galaxy is measured where its radially averaged H I surface density reaches the 1 $M_\odot/pc^2$ level, and its optical isophotal diameter R_{25} is based on D_{25} measured at the 25 mag arcsec^{-2} level in the B band. To determine $r_{\rm max}$ we adopted the following average ratios for the H I-to-optical radii: 2.5±1.1 for LSB galaxies (de Blok et al. 1996) and 1.6±0.3 for HSB galaxies (Rhee & van Albada 1996).

6. Conclusions

We estimated the dark matter contents of eight galaxies using 21cm H I line spectra we obtained with the single-dish NRT. We found that the estimated dark matter component dominates their total mass at the 85% level, a result which is consistent with other estimates (e.g., de Blok et al. 1996; Rhee & van Albada 1996).

The main sources of uncertainty in our dark matter mass estimates are (1) that the 3D distribution of dark matter around galaxies is not (well) known, which led to our use of an overly simplified formula for the estimation of the total mass (as other studies have done, perforce), and (2) the H I distribution radius $r_{\rm max}$, estimated based on average values measured from interferometric H I line imaging of other galaxies.

References

Aihara, H., Allende Prieto, C., An, D., et al. 2011, ApJS, 193, 29
Alam, S., Albareti, F. D., Allende Prieto, C., et al. 2015, ApJS, 219, 12
Allen, C. W. 1973, Astrophysical quantities
Blackman, C. P. & Pence, W. D. 1982, MNRAS, 198, 517
Cardelli, J. A., Clayton, G. C., & Mathis, J. S. 1989, ApJ, 345, 245
de Blok, W. J. G., McGaugh, S. S., & van der Hulst, J. M. 1996, MNRAS, 283, 18
Karachentsev, I. D., Karachentseva, V. E., & Parnovskij, S. L. 1993, Astronomische Nachrichten, 314, 97
Matthews, L. D. 2000, The Astronomical Journal, 120, 1764
Matthews, L. D. & Uson, J. M. 2008, AJ, 135, 291
Matthews, L. D. & van Driel, W. 2000, A&AS, 143, 421
McGaugh, S. S., Schombert, J. M., Bothun, G. D., & de Blok, W. J. G. 2000, The Astrophysical Journal, 533, L99
O'Neil, K., Bothun, G., van Driel, W., & Monnier Ragaigne, D. 2004, A&A, 428, 823
Rhee, M. H. & van Albada, T. S. 1996, A&AS, 115, 407
Schlafly, E. F. & Finkbeiner, D. P. 2011, ApJ, 737, 103
Schneider, S. E., Thuan, T. X., Magri, C., & Wadiak, J. E. 1990, ApJS, 72, 245
van Driel, W., Butcher, Z., Schneider, S., et al. 2016, A&A, 595, A118